VIP Lithium Oxides Very Important Paper

International Edition: DOI: 10.1002/anie.201900444
German Edition: DOI: 10.1002/ange.201900444

Stabilizing the Oxygen Lattice and Reversible Oxygen Redox Chemistry through Structural Dimensionality in Lithium-Rich Cathode Oxides

Enyue Zhao[+], Qinghao Li[+], Fanqi Meng[+], Jue Liu, Junyang Wang, Lunhua He, Zheng Jiang, Qinghua Zhang, Xiqian Yu, Lin Gu,* Wanli Yang,* Hong Li, Fangwei Wang,* and Xuejie Huang*

Abstract: *Lattice-oxygen redox (l-OR) has become an essential companion to the traditional transition-metal (TM) redox charge compensation to achieve high capacity in Li-rich cathode oxides. However, the understanding of l-OR chemistry remains elusive, and a critical question is the structural effect on the stability of l-OR reactions. Herein, the coupling between l-OR and structure dimensionality is studied. We reveal that the evolution of the oxygen-lattice structure upon l-OR in Li-rich TM oxides which have a three-dimensional (3D)-disordered cation framework is relatively stable, which is in direct contrast to the clearly distorted oxygen-lattice framework in Li-rich oxides which have a two-dimensional (2D)/3D-ordered cation structure. Our results highlight the role of structure dimensionality in stabilizing the oxygen lattice in reversible l-OR, which broadens the horizon for designing high-energy-density Li-rich cathode oxides with stable l-OR chemistry.*

Owing to the attainable ultrahigh capacity, lithium-rich transition-metal oxides have attracted wide attention as candidates for the cathode in high-energy-density Li-ion batteries.[1] It has been reported that the anomalously high capacity in these materials originates from the cumulative redox of TMs and lattice oxygen.[2] Unlike the TM redox chemistry, the lattice-oxygen redox (l-OR) is more intricate and its mechanism is yet to be clarified. Additionally, it seems that the oxygen redox activities may cause detrimental effects (e.g., irreversible structure transition) on the electrochemical performance.[3] At this time, in-depth characterizations of the l-OR chemistry as well as guidelines for achieving its stable operation are still required.

In Li-rich cathode oxides, the presence of Li-O-Li units with unhybridized O 2p orbitals was proposed to be responsible for their l-OR activity.[4] Thus, the l-OR behavior is closely associated with the spatial distribution and orientation (which is directly correlated with the structure dimensionality) of the Li-O-Li units (unhybridized O 2p orbital) in the overall structure.[4] For example, in Li-rich layered oxides, the unhybridized O 2p orbitals are orderly distributed in the framework owing to the 2D-ordered (e.g., honeycomb structure) TM/Li layer structure of the compound (Scheme 1 a, Scheme S1 in the Supporting Information). It has been reported that the l-OR in these materials can be controlled by introducing stacking faults which can alter the structure dimensionality along the vertical direction of the TM/Li layer and thus affect the configuration of unhybridized O 2p orbitals.[5] Furthermore, l-OR chemistry was also detected in Li-rich layered oxides with 3D-ordered TM/Li frameworks.[6] It is clear that the structural dimensionality will affect the l-OR and define the electrochemical performance.

Nevertheless, to date, how the structure dimensionality affects the l-OR and how to employ such an effect to design a better Li-rich cathode oxide with stable l-OR remain open questions. Therefore, l-OR needs to be studied in Li-rich cathode oxides with a structural dimensionality different from that of the Li-rich layered compounds. For such a comparative study, the cation-disordered Li-rich oxides with a 3D-disordered cationic framework (Scheme 1 b) are a perfect candidate.[7] Herein, we reveal the coupling relationship between l-OR and structure dimension in cation-disordered Li-rich oxide $Li_{1.2}Ti_{0.35}Ni_{0.35}Nb_{0.1}O_{1.8}F_{0.2}$ (LTNNbOF). Our results suggest that the structure dimensionality can be utilized effectively to design high-performance cathode oxides with stable l-OR.

Pure-phase LTNNbOF (Figures S1, S2) was prepared by a solid-state calcination method. Refinement results of the

[*] E. Zhao,[+] Dr. Q. Li,[+] F. Meng,[+] J. Wang, Prof. L. He, Dr. Q. Zhang, Prof. X. Yu, Prof. L. Gu, Prof. H. Li, Prof. F. Wang, Prof. X. Huang
Institute of Physics, Chinese Academy of Sciences
Beijing 100190 (China),
and
School of physical sciences, University of Chinese Academy of Sciences
Beijing 100049 (China),
and
Songshan Lake Materials Laboratory
Dongguan, Guangdong 523808 (China)
E-mail: xyu@iphy.ac.cn
l.gu@iphy.ac.cn
fwwang@iphy.ac.cn
Dr. W. Yang
Advanced Light Source, Lawrence Berkeley National Laboratory
Berkeley, CA 94720 (USA)
E-mail: WLYang@lbl.gov
Dr. J. Liu
Neutron Scattering Division, Oak Ridge National Laboratory
Oak Ridge, TN 37831 (USA)
Dr. Z. Jiang
Shanghai Synchrotron Radiation Facility
Shanghai, 201204 (China)
[+] These authors contributed equally to this work.
Supporting information and the ORCID identification number(s) for the author(s) of this article can be found under: https://doi.org/10.1002/anie.201900444.

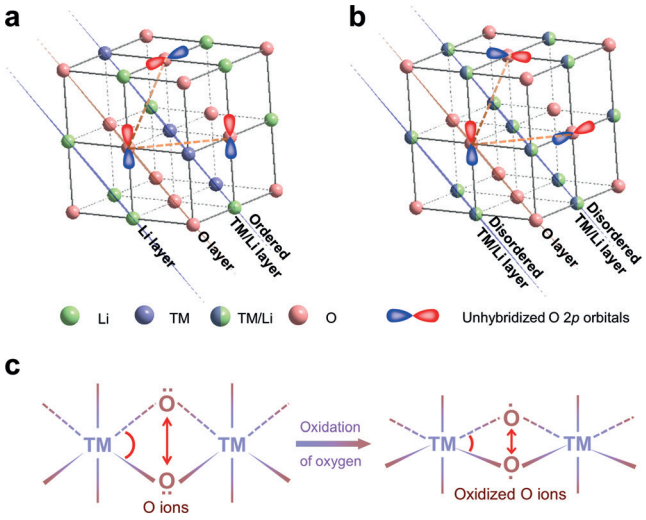

Scheme 1. a) 2D-ordered cation layer for Li-rich TM oxides with coplanar unhybridized O 2p orbitals in the interlayer; b) 3D-disordered cation framework for Li-rich TM oxides with a random spatial distribution of unhybridized O 2p orbitals; c) Schematic representation of the shrinking distance between a pair of O–O ions and the corresponding structure distortion.

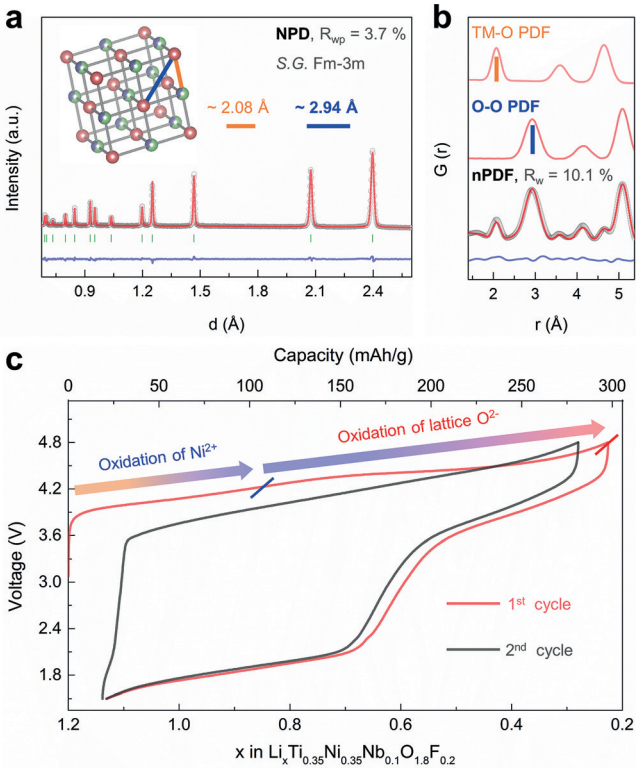

Figure 1. Refinement results of the a) neutron powder diffraction (NPD), and b) neutron pair distribution function (nPDF) patterns. Inset in (a) shows the crystal structure of LTNNbOF, the distances between the pairs of atoms with corresponding PDF peaks are labeled in (b); c) The voltage profiles of the first two cycles for LTNNbOF at 20 mA g^{-1}. See also Figure S3, S4.

neutron powder diffraction (NPD) pattern confirmed its (*S.G.*) $Fm\bar{3}m$ cation-disordered rock-salt structure (Figure 1 a, Table S1), which can be simply described as that all the cations (TM/Li) distribute randomly in the anionic 3D-framework with the oxygen atoms occupying octahedral sites (inset in Figure 1 a). The nearest-neighbor TM–O (e.g., Ni–O) distance (ca. 2.08 Å) and O–O distance (ca. 2.94 Å) are refined from the local neutron pair distribution function (nPDF) patterns (Figure 1 b, Table S2).

The electrochemical performance of LTNNbOF is shown in Figure 1 c, in which an initial charge capacity of approximately 300 mA h g^{-1} (equivalent to ca. 0.97 Li extraction) and a high reversible discharge capacity of approximately 277 mA h g^{-1} (corresponding to ca. 0.91 Li re-insertion) were obtained. Considering the theoretical capacity of approximately 214 mA h g^{-1} based on the Ni^{2+}/Ni^{4+} redox couple as well as the electrochemical inertness of Ti^{4+}, Nb^{5+}, F^- ions, l-OR needs to be naturally invoked for the charge compensation mechanism, which is experimentally clarified below through soft X-ray absorption spectroscopy (sXAS) and mapping of resonant inelastic X-ray scattering (mRIXS).

TM L-edges directly probe the 3d valence states through excitations of 2p electrons to 3d orbitals, which provides the sensitivity to quantitatively determine the TM oxidation states.[8] As shown in Figure 2 b,c, partial Ni^{2+} ions were oxidized to Ni^{3+} and Ni^{4+} ions upon charging up to 4.3 V, and during the subsequent charging process, the oxidation states of the Ni ions remains relatively stable. For the F^-, Ti^{4+} and Nb^{5+} ions, there is no observable evidence that they participate in the charge compensation (Figure S6–8).[9] This quantitative analysis indicates that the charge compensation in LTNNbOF is mainly from l-OR during charging from 4.3 V to 4.8 V.

Direct evidence of the l-OR in LTNNbOF could be revealed through oxygen spectroscopy. First, the pre-edge features of sXAS changes in lineshape and enhances in intensity upon charging (Figure S9). However, these evolutions are due to the changes in TM states and TM-O hybridization strength.[8a] Second, compared with the pristine state (Figure 2 d), O-*K* mRIXS of the 4.8 V charged electrode shows enhanced intensity at 523.7 eV emission and 531 eV excitation energies (white arrow in Figure 2 e). It has been established that an enhanced mRIXS feature here is a signature of partially occupied O-2p bands in non-divalent oxygen, that is, oxidized oxygen,[10] thus providing a reliable fingerprint of l-OR states in charged electrodes.[8a] Indeed, Figure 2 f shows the integrated mRIXS intensity around 531 eV excitation energy, which displays a gradual enhancement of the intensity at 523.7 eV (shaded range) during charging, indicating oxidized oxygen in the charged electrodes at high potentials. Note that well isolated l-OR mRIXS feature has been found in various charged electrodes including Li-rich layered oxides,[8a] but charged LTNNbOF displays only an enhanced shoulder feature here. This is mainly due to the overlapping of l-OR and Ti-O hybridization features at exactly the same excitation energy at 531 eV, leading to only a shoulder, instead of an isolated feature, of the l-OR signals in LTNNbOF. Nonetheless, the systematic evolution of the 523.7 eV shoulder in Figure 2 f upon cycling reveals the l-OR

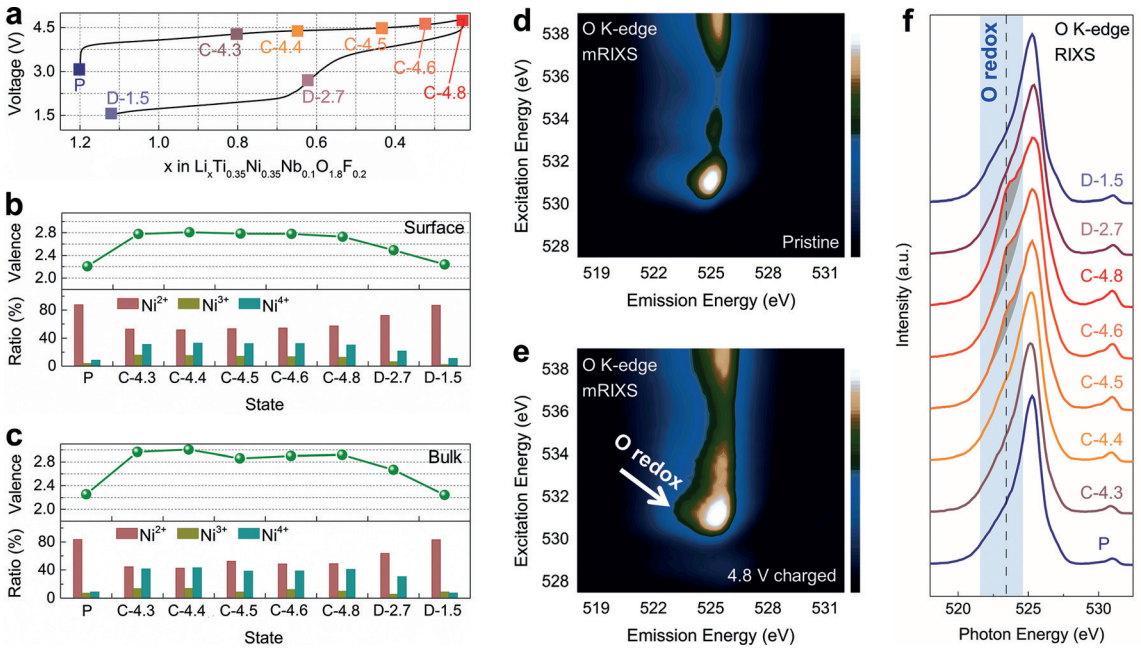

Figure 2. a) The initial electrochemical cycle curve at 20 mA g^{-1}. b) Surface and c) bulk valence evolution of Ni ions (top panel) as well as the ratio variation of the different-valence Ni ions (bottom panel) based on the fitted Ni L-edge sXAS spectra in Figure S5. The mRIXS results of the d) pristine and e) 4.8 V charged electrodes. f) The ex situ RIXS spectra of the O K-edge, see text for details. See also Scheme S2.

reactions in LTNNbOF, and more importantly, the intensity drops in the following discharging, indicating a reversible l-OR activity.

It has been reported that the storage of charge (or electron) on the lattice oxygen ions can alter their electronic structure, which will further affect the oxygen lattice framework (i.e., O–O atomic-pair distance).[4] Thus, nPDF, capable of highlighting the oxygen scattering and analyzing the atomic-pair coordination, was employed to directly reveal the variation of O–O distance in the bulk structure of LTNNbOF upon Li de-/re-intercalation process. Surprisingly, no obvious change of the average O–O distance in LTNNbOF was observed during the electrochemical cycling (Figure 3a and Figure S10). The broad PDF peaks upon cycling may be correlated with the local variation of cations content and also due to the resolution of the diffractometer, and more accurately quantitative analysis will be done using higher resolution instrument. The relative stable oxygen lattice was further verified by atomic-resolution scanning transmission electron microscopy (STEM) which can clearly present the projection of oxygen columns along the [110] axis without overlapping with the columns of TM or Li in LTNNbOF (Figure 3b,c). High-angle annular dark field (HAADF) STEM images in Figure 3b,c shows the almost invariant average distance among the oxygen columns projected along the [110] axis from the pristine to high-charged state. The phenomenon observed in cation-disordered Li-rich oxides with 3D-disordered cation framework is very different from the distorted TM-O octahedron with significantly shortened O-O pair distance

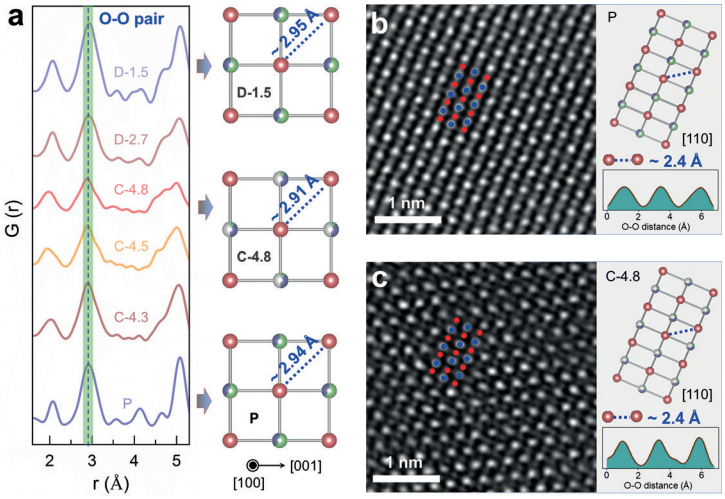

Figure 3. a) The ex situ local nPDF patterns (left panel), and variation of the average O–O distance (right panel). [110] STEM-HAADF images of the b) pristine and c) 4.8 V charged samples, the corresponding average distances of the nearest-neighbor O–O columns projected along the [110] axis are labeled in the structure schematic. See average structure analysis in Figure S11.

detected in Li-rich oxides with either 2D-ordred cation layer or 3D-ordered cation framework.[2d,6]

The contrast in the oxygen lattice stability in these Li-rich oxides could be understood by considering their different dimensional configurations and unhybridized O 2p orbital configurations (or orientation). The electronic storage (or the production of electronic holes) usually occurs on the lattice O^{2-} ions with Li-O-Li coordination upon l-OR. To reduce the energy of the oxidized O^{2-} ions (denoted as O^{-}), the interaction between two O^{2-} is enhanced by decreasing the

O–O pair distance, which will result in the decrease of O-TM-O angle and overlap between TM e_g orbitals and O 2p orbitals. This weakens the TM−O bonding and is not favorable for the stabilization of the structure framework (Scheme 1 c). In the meantime, the decrease of O–O distance is closely associated with the directional-distribution correlation between two unhybridized O 2p orbitals. The O–O distance would not obviously decrease if the two unhybridized O 2p orbitals are non-coplanar, because there is insufficiently interaction or bonding trend between them. The O–O distance would significantly decrease only when the corresponding unhybridized O 2p orbitals are coplanar.

For Li-rich cathode oxides with 2D-ordered cation layer, there are coplanar unhybridized O 2p orbitals in the TM interlayer (Scheme 1 a) and non-coplanar unhybridized O 2p orbitals in the TM intralayer (Scheme S1) due to the ordered spatial distribution of cations. In the oxidized state, the oxidized O–O pairs with coplanar unhybridized O 2p orbitals would shorten their distance to reduce the energy. In contrast, for Li-rich cathode oxides with 3D-disordered cation framework (Scheme 1 b), the spatial correlation between two unhybridized O 2p orbitals is disordered (random), which greatly reduce the formation probability of coplanar unhybridized O 2p orbitals. This situation makes the coplanar unhybridized O 2p orbitals, if any, randomly distribute in the structure framework. In this case, the original O-TM-O bonding-structure framework is more likely to be maintained, rather than clearly distorted during the l-OR process. Thus, no notable variation of the average O–O distance was found in LTNNbOF with such a 3D-disordered cation framework. (Figure 3, Figure S10–12) We note that a relatively well-preserved oxygen lattice framework is important to stabilize the reversible l-OR against other irreversible oxygen activities upon electrochemical operations.

The finding of relatively stable oxygen lattice structure framework in the 3D-disordered LTNNbOF system, contrasting that in Li-rich layered systems, suggests that dimensional configurations could be utilized to achieve both reversible l-OR and a stable structure upon electrochemical cycling. Usually, the structure transition (e.g., distortion of TM-O octahedron, gliding of TM layer, TM migration) in Li-rich cathode oxides with 2D-ordered structure is common upon l-OR, and this transition behavior would be irreversible once there is the loss of O_2 gas.[11] The irreversible structure transition may further induce the unstable l-OR, leading to detrimental effects in electrochemical performance (e.g., voltage fade, capacity degradation).[12] Such effects do not take place in a 3D-disordered structure because of its relatively robust oxygen lattice structure framework even with active l-OR reactions (Figure 3). The relatively inferior cycle life in the reported 3D-disordred-structure samples may be correlated with their intrinsically limited Li de-/re-intercalated kinetics upon cycling and/or the electrode surface/interface degradation, which is briefly discussed in the Supporting Information and is beyond the scope of this work. Herein, we propose that the structure dimensionality can be utilized as an optimization parameter for achieving high energy density with stable l-OR in Li-rich cathode oxides. For instance, 1) the localized 3D-disordered structure dimensions can be redesigned into the framework of practical Li- and Mn-rich layered oxides (with 2D-ordered structure) to improve their oxygen lattice stability; 2) a Li-rich oxide particle with a gradient of structure-dimensionality could be constructed to achieve both the stable l-OR and facile Li-(de)intercalated kinetics.

In summary, the structural-dimensionality effect on the l-OR and associated oxygen lattice stability in Li-rich cathodes have been characterized and clarified. In contrast to the Li-rich TM oxides with 2D-ordered cation structure, the Li-rich TM oxides with 3D-disordered cation framework show a relatively stable oxygen lattice structure accompanying the l-OR. We explain this finding based on the different spatial-distribution of unhybridized O 2p orbitals in the different structure dimensionality. This work suggests that the structure dimensionality can be designed and employed to promote reversible l-OR with a stable structure in Li-rich cathode oxides. More importantly, the findings reveal the critical structural-dimensionality effects on l-OR and its related oxygen lattice structure, paving new ways in both academic research and practical developments of high-energy-density cathodes relying on stable l-OR chemistry.

Acknowledgements

This work was supported by funding from National Key R&D Program of China (2016YFA0202500), Foundation for Innovative Research Groups of the NSFC (No. 51421002), NSFC (No. 11675255, 51502334, 51822211). This work used resources of the ALS, which is a US DOE Office of Science User Facility, W.Y. acknowledges support from EERE VTO under the Applied Battery Materials Program of the US DOE, both under Contract No. DE-AC02-05CH11231.

Conflict of interest

The authors declare no conflict of interest.

Keywords: cathodes · lattice oxygen redox · lithium-ion batteries · oxides · structural dimensionality

How to cite: *Angew. Chem. Int. Ed.* **2019**, *58*, 4323 – 4327
Angew. Chem. **2019**, *131*, 4367 – 4371

[1] a) J.-L. Shi, D.-D. Xiao, M. Ge, X. Yu, Y. Chu, X. Huang, X.-D. Zhang, Y.-X. Yin, X.-Q. Yang, Y.-G. Guo, L. Gu, L.-J. Wan, *Adv. Mater.* **2018**, *30*, 1705575; b) H. Yu, H. Zhou, *J. Phys. Chem. Lett.* **2013**, *4*, 1268 – 1280; c) J. Liu, M. Hou, J. Yi, S. Guo, C. Wang, Y. Xia, *Energy Environ. Sci.* **2014**, *7*, 705 – 714.

[2] a) C. Delmas, *Nat. Chem.* **2016**, *8*, 641 – 643; b) B. Li, D. Xia, *Adv. Mater.* **2017**, *29*, 1701054; c) X. Li, Y. Qiao, S. Guo, Z. Xu, H. Zhu, X. Zhang, Y. Yuan, P. He, M. Ishida, H. Zhou, *Adv. Mater.* **2018**, *30*, 1705197; d) E. McCalla, A. M. Abakumov, M. Saubanere, D. Foix, E. J. Berg, G. Rousse, M.-L. Doublet, D. Gonbeau, P. Novak, G. Van Tendeloo, R. Dominko, J.-M. Tarascon, *Science* **2015**, *350*, 1516 – 1521.

[3] a) W. Yang, *Nat. Energy* **2018**, *3*, 619 – 620; b) E. Hu, X. Yu, R. Lin, X. Bi, J. Lu, S. Bak, K.-W. Nam, H. L. Xin, C. Jaye, D. A. Fischer, K. Amine, X.-Q. Yang, *Nat. Energy* **2018**, *3*, 690 – 698.

[4] D.-H. Seo, J. Lee, A. Urban, R. Malik, S. Kang, G. Ceder, *Nat. Chem.* **2016**, *8*, 692 – 697.
[5] R. Shunmugasundaram, R. S. Arumugam, J. R. Dahn, *J. Electrochem. Soc.* **2016**, *163*, A1394 – A1400.
[6] P. E. Pearce, A. J. Perez, G. Rousse, M. Saubanere, D. Batuk, D. Foix, E. McCalla, A. M. Abakumov, G. Van Tendeloo, M.-L. Doublet, J.-M. Tarascon, *Nat. Mater.* **2017**, *16*, 580 – 586.
[7] a) J. Lee, A. Urban, X. Li, D. Su, G. Hautier, G. Ceder, *Science* **2014**, *343*, 519 – 522.
[8] a) W. Yang, T. P. Devereaux, *J. Power Sources* **2018**, *389*, 188 – 197; b) Q. Li, R. Qiao, L. A. Wray, J. Chen, Z. Zhuo, Y. Chen, S. Yan, F. Pan, Z. Hussain, W. Yang, *J. Phys. D* **2016**, *49*, 413003.
[9] a) N. Yabuuchi, M. Nakayama, M. Takeuchi, S. Komaba, Y. Hashimoto, T. Mukai, H. Shiiba, K. Sato, Y. Kobayashi, A. Nakao, M. Yonemura, K. Yamanaka, K. Mitsuhara, T. Ohta, *Nat. Commun.* **2016**, *7*, 13814 – 13823 ; b) E. Zhao, L. He, B. Wang, X. Li, J. Zhang, Y. Wu, J. Chen, S. Zhang, T. Liang, Y. Chen, X. Yu, H. Li, L. Chen, X. Huang, H. Chen, F. Wang, *Energy Storage Mater.* **2019**, *16*, 354 – 363.
[10] Z. Zhuo, C. D. Pemmaraju, J. Vinson, C. Jia, B. Moritz, I. Lee, S. Sallies, Q. Li, J. Wu, K. Dai, Y. D. Chuang, Z. Hussain, F. Pan, T. P. Devereaux, W. Yang, *J. Phys. Chem. Lett.* **2018**, *9*, 6378 – 6384.
[11] a) X.-D. Zhang, J.-L. Shi, J.-Y. Liang, Y.-X. Yin, J.-N. Zhang, X.-Q. Yu, Y.-G. Guo, *Adv. Mater.* **2018**, *30*, 1801751; b) H. Yu, R. Ishikawa, Y.-G. So, N. Shibata, T. Kudo, H. Zhou, Y. Ikuhara, *Angew. Chem. Int. Ed.* **2013**, *52*, 5969 – 5973; *Angew. Chem.* **2013**, *125*, 6085 – 6089.
[12] a) R.-P. Qing, J.-L. Shi, D.-D. Xiao, X.-D. Zhang, Y.-X. Yin, Y.-B. Zhai, L. Gu, Y.-G. Guo, *Adv. Energy Mater.* **2016**, *6*, 1501914; b) B. Qiu, M. Zhang, L. Wu, J. Wang, Y. Xia, D. Qian, H. Liu, S. Hy, Y. Chen, K. An, Y. Zhu, Z. Liu, Y. S. Meng, *Nat. Commun.* **2016**, *7*, 12108 – 12117; c) B. Qiu, M. Zhang, Y. Xia, Z. Liu, Y. S. Meng, *Chem. Mater.* **2017**, *29*, 908 – 915.

Manuscript received: January 11, 2019
Accepted manuscript online: February 1, 2019
Version of record online: February 19, 2019

